Preprints of the 21st IFAC World Congress (Virtual)
Berlin, Germany, July 12-17, 2020

Visual-Detection based Fruit Fly Optimization Algorithm for Robust Analysis of Integrated Energy Systems

Weizhen Hou *, Jiayu Li *, Jing Xu *, Kwang Y. Lee **, Yu Huang *

**Department of Automation, North China Electric Power University, Baoding 071003, China;*
***Department of Electrical &Computer Engineering, Baylor University, Waco, TX 76798, USA (Correspondence: Kwang_Y_Lee@baylor.edu; Tel.: +001- (254) 710-4188)*

Abstract: In this paper, a visual-detection (VD)-based fruit fly optimization algorithm (FOA) is proposed for solving a robust analysis problem of integrated energy systems (IES) with energy storage based on the information gap decision theory (IGDT). In the searching phase, the VD-based decision delay and visual feature detection are incorporated within the FOA. VD-FOA changes the search radius of fruit fly according to the variance of smell concentration, which can solve the problem that fruit fly optimization algorithm is easy to fall into local optimization, where standard test functions are also adopted to test the proposed algorithm. The proposed VD-FOA is superior to the basic FOA and is applied to solve the IGDT-based robust analysis problem of IES with energy storage. The simulation results show the applicability and effectiveness of the proposed algorithm.

Keywords: smart grids; control of renewable energy resources; power systems stability; intelligent control of power systems; optimal operation and control of power systems

1. INTRODUCTION

An integrated energy system (IES) is a coupled energy system that comprehensively utilizes electricity, gas, heat and other forms of energy to effectively promote the local consumption of renewable energies and to improve energy utilization (Stanislav,P et al,2009). However, the accessibility of wind power greatly affects the robustness of the IES. The present methods for the robust analysis of energy systems mainly include stochastic programming (Vahid-Pakdel, M. J, 2017.Tabar, V. S, 2017), fuzzy decision theory (Mombeini, H, 2018) and robust optimization (Xiong, P, 2016.Alismail, F, 2018). Although the above methods provide effective references for robust analysis of energy systems, wind power, given its serious uncertainty, cannot provide a precise probability distribution or membership functions of uncertain variables for traditional robust analysis methods, thereby imposing challenges to the robust analysis of IES.

Proposed by Haim in 2006, information gap decision theory (IGDT) presents a new approach for dealing with uncertainties (Ben-Haim, Y,2006). Compared with stochastic programming, fuzzy decision theory and robust optimization, IGDT has better applicability and does not require the probability density function of uncertain parameters or the related membership function. The IGDT has been recently applied in uncertainty research, such as (Dolatabadi, A,2019. Rabiee, A, 2018.). IGDT was applied to build the uncertainty of electrical load (Nojavan, S,2017). To determine the bidding strategy of a renewable microgrid, the price uncertainty of the upstream power grid was modelled by using IGDT (Mehdizadeh, A,2018). Accordingly, a robust analysis model of IES was built in this paper by using IGDT.

An IES with wind power contains many energy conversion equipment that can result in the large dimension of an IES robust analysis model, thereby making this model difficult to solve. Accordingly, scholars have proposed several methods to solve this problem, such as the particle swarm optimization (PSO) and the genetic algorithm (GA) (Kampouropoulos, K,2018). To solve the optimal power flow of an IES with a renewable distributed access, (Khaled, U,2017) incorporated a modified smart technique that uses PSO. To schedule the unit commitment and economic dispatch of microgrid units, (Nemati, M, 2018) developed an improved real- coded genetic algorithm. However, compared with GA and PSO, the application of fruit fly optimization algorithm (FOA) in solving the problem of the IES robust analysis is fewer.

The FOA proposed in (Shudapreyaa, R, 2015) is a simple and feasible algorithm that has attracted great interest and got extensive application. An innovative prediction model based on generalized regression neural network and FOA was developed in (Niu, D ,2017). A multi-objective model of FOA was proposed in (El-Ela, A. A. A,2018) to effectively solve the optimal power flow problem, an improved FOA was proposed in (Darvish, A,2018) to solve the synthetic antenna array problem and a modified FOA was built in (Dongxiao, N,2017) for medium- and long-term load forecasting and has been proven effective and feasible. However, FOA is rarely used in robust analysis of IES since can easily fall into local optimization and cannot easily achieve the ideal convergence accuracy. Therefore, this paper proposes a visual-detection (VD)-based FOA, which changes the search radius of fruit fly algorithm in the process of optimization in order to avoid falling into local optimization in the process of convergence.

In this paper, the IES robust analysis model proposed in this work was built by using IGDT and solved by using VD-FOA. The influence of the energy storage (ES) unit and its maximum state of charge (SOC) on the robustness of the system was also examined. The rest of this paper is organized as follows. Section 2 presents the IGDT robust analysis model of IES. Section 3 presents the VD-FOA and analyzes its performance. Section 4 presents some case studies and Section 5 concludes the paper.

2. IGDT ROBUST ANALYSIS MODEL OF IES

2.1 Integrated Energy Systems Model

The schematic diagram of an IES is presented in Fig. 1. The IES model mainly includes a power grid, natural gas network and related equipment.

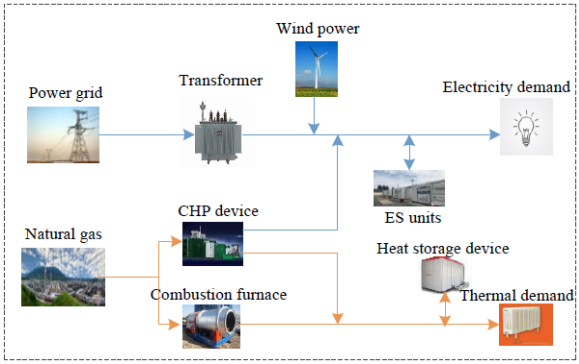

Fig. 1. Schematic diagram of an integrated energy system (IES).

2.1.1 Power grid model

The power grid model includes the system power balance equation and the limitation of branch transmission power, which can be computed as

$$\sum_{g\in\Omega_i} P_{g,t} + P^{w}_{i,t} - L_{i,t} + P^{d}_{i,t} - P^{c}_{i,t} = \sum_{j\in\Omega_i} P_{ij,t} \tag{1}$$

$$P_{ij,t} = \frac{V^{2}_{i,t}}{Z_{ij}}\cos\left(\theta_{ij}\right) - \frac{V_{i,t}V_{j,t}}{Z_{ij}}\cos\left(\delta_{i,t} - \delta_{j,t} + \theta_{ij}\right) \tag{2}$$

$$-P^{max}_{ij} \le P_{ij,t} \le P^{max}_{ij,t} \tag{3}$$

In equation (1), $P_{g,t}$ and $P^{w}_{i,t}$ denote the outputs of energy unit and wind farm, respectively, $L_{i,t}$ denotes the electrical load, $P^{c}_{i,t}$ and $P^{d}_{i,t}$ denote the battery charging and discharging powers, respectively, and $P_{ij,t}$ represents the transmission power. Meanwhile, in equation (2), $V_{i,t}$ and $\delta_{i,t}$ denote the voltage magnitude and phase angle, respectively, Z_{ij} and θ_{ij} denote the impedance magnitude and phase angle, respectively. Equation (3) represents the transmission line power limit, where $P^{\max}_{ij,t}$ represents the maximum transmission line power.

2.1.2 Natural gas network model

The natural gas flow balance equation, pipeline flow constraint and node pressure constraint are all present in the following natural gas network model:

$$\sum_{j} f_{i,j,t} = \sum_{j} f_{j,i,t} + Sg_{i,t} - \xi_{g,t}Sd_{i} - Se_{i,t} \tag{4}$$

$$f_{j,i,t} = C_{j,i}\sqrt{Pr^{2}_{j,t} - Pr^{2}_{i,t}} \tag{5}$$

$$f_{j,i,t} \ge C_{j,i}\sqrt{Pr^{2}_{j,t} - Pr^{2}_{i,t}} \tag{6}$$

$$Sg^{min}_{i} \le Sg_{i,t} \le Sg^{max}_{i} \tag{7}$$

$$Pr^{min}_{i} \le Pr_{i,t} \le Pr^{max}_{i} \tag{8}$$

where $f_{j,i,t}$ represents the natural gas flow, $Sg_{i,t}$ is the injected natural gas flow, Sd_i represents the maximum natural gas flow for supply, $\zeta_{g,t}$ denotes the standard unitary value of natural gas flow demand and $Se_{i,t}$ represents the combined heat and power (CHP) unit demand for natural gas flow. Equations (5) and (6) denote the non-adjustable and adjustable pressure node constraints, where P_r represents the node pressure and $C_{i,t}$ represents the pipe coefficient that is related to temperature, length, diameter and friction. Equations (7) and (8) represent the upper/lower limits of natural gas flow and node pressure, respectively.

2.1.3 Device model

2.1.3.1 Energy storage unit model

According to the law of energy conservation, the ES unit model can be formulated as

$$SOC_{i,t} = SOC_{i,t-1} + (P^{c}_{i,t}\eta_{c} - P^{d}_{i,t}/\eta_{d})E_{i,max} \tag{9}$$

$$SOC_{i,t} = \frac{E_{i,t}}{E_{i,max}} \tag{10}$$

$$P^{c,min}_{i} \le P^{c}_{i,t} \le P^{c,max}_{i} \tag{11}$$

$$P^{d,min}_{i} \le P^{d}_{i,t} \le P^{d,max}_{i} \tag{12}$$

$$SOC_{i,min} \le SOC_{i,t} \le SOC_{i,max} \tag{13}$$

In equation (9), η_c and η_d denote the battery charging and discharging efficiencies, respectively, and $E_{i,max}$ denotes the maximum capacity of the battery. In equation (10), $E_{i,t}$ denotes the stored energy of the battery, equations (11) and (12) are for the upper and lower limits of battery charging/discharging power, respectively, and equation (13) are for the upper and lower limits of the state of charge (SOC) of the battery.

2.1.3.2 Unit output power model

The unit output power includes the conventional unit and the CHP unit output whereas its model mainly includes the gas-electricity conversion equation and the unit power output limit. This model is formulated as

$$Se_{i,t} = \eta_{G2P}P^{g}_{i,t} \tag{14}$$

$$P^{g}_{i,t} - P^{g}_{i,t-1} \le RU_{g} \tag{15}$$

$$P^{g}_{i,t-1} - P^{g}_{i,t} \le RD_{g} \tag{16}$$

$$P^{g,min}_{i} \le P^{g}_{i,t} \le P^{g,max}_{i} \tag{17}$$

In the gas-electricity conversion equation (14), $P^{g}_{i,t}$ denotes the unit power output and η_{G2P} represents the conversion efficiency coefficient of CHP. Meanwhile, equations (15) and (16) are for the ramp-up/down limits of unit output power, where RU_g and RD_g represent the upper limits of the ramp-

up/down of unit power output, respectively. Equation (17) represents the unit power output limit.

2.1.4 Analysis of IES operating cost

The operating costs of IES mainly include conventional unit power generation costs and natural gas costs and can be mathematically expressed as

$$f = EC + GC \tag{18}$$

where EC is the cost of power generation for conventional units and GC indicates the cost of natural gas. Generally, the generation cost of a conventional unit can be expressed as a quadratic function of output power as follows:

$$EC = \sum_{g,t}\left(a_g(P_{g,t})^2 + b_g P_{g,t} + c_g\right) \tag{19}$$

where a_g, b_g and c_g denote the cost coefficients of conventional units and $P_{g,t}$ indicates the output power of conventional units. The natural gas cost can be expressed as follows:

$$GC = \sum_{i,t} C_i Sg_{i,t} \tag{20}$$

where C_i is the natural gas price coefficient. Nevertheless, wind power access brings strong uncertainty to the system, thereby preventing the system from satisfying the needs of users or the network constraints. Therefore, the robustness of IES with wind power must be analyzed. This paper establishes a robust model of IES by using IGDT.

2.2 Robust Model of Information Gap Decision Theory IGDT

The traditional methods for solving uncertainty have a high computational burden and depend on the membership or probability density function of uncertain variables. Given that uncertainty problems cannot be accurately modelled as historical data, therefore this study applied IGDT to build a robust analysis model for IES with wind power.

2.2.1. IGDT

This section introduces IGDT, which can effectively solve the uncertainty of wind power in an IES. In general, the optimization model of an IES can be expressed as

$$\begin{cases} f = \max\limits_{x}(f(X,\gamma)) \\ s.t. \quad H(X,\gamma) \le 0 \\ \qquad G(X,\gamma) = 0 \end{cases} \tag{21}$$

where f indicates the objective function, X represents a set of decision variables, γ represents the vector of input parameters and H and G denote the inequality and equality constraints of the decision variable X, respectively. Assuming that the predicted value of the parameter is $\tilde{\gamma}$ and that γ is random in practice, the uncertainty set can be mathematically expressed as

$$\forall \gamma \in U(\tilde{\gamma},\alpha) = \left\{\gamma : \left|\frac{\gamma - \tilde{\gamma}}{\tilde{\gamma}}\right| \le \alpha\right\} \tag{22}$$

where α represents the radius of uncertainty, that is, the maximum deviation between the true and predicted values of the uncertain parameter.

When $\gamma = \tilde{\gamma}$, the optimal solution f_0 of model (24) can be obtained. However, having an uncertain parameter can introduce fluctuations in the predicted value and the decision maker sets an acceptable maximum cost based on experience. Therefore, the following constraint needs to be added to the optimization model:

$$f_r = (1+\beta) f_0, \quad \beta \ge 0 \tag{23}$$

In equation (23), β represents the deviation factor that is defined as the percentage increase in the objective function. In sum, the robust optimization model built based on IGDT can be expressed as

$$\begin{cases} \max\limits_{X} \alpha \\ s.t. \quad f \le (1+\beta) f_0 \\ \qquad H(X,\gamma) \le 0 \\ \qquad G(X,\gamma) = 0 \\ \qquad \forall \gamma \in U(\alpha,\tilde{\gamma}), \quad 0 \le \alpha \le 1 \end{cases} \tag{24}$$

In this model, when the objective function value f is lower than the highest expected objective f_r, the maximum fluctuation amplitude α of the uncertain parameters can be obtained.

2.2.2. Robust model of IGDT

According to equation (22), the fluctuation range of uncertain wind farm output can be expressed as

$$U\left(\alpha,\ \tilde{P}_{i,t}^{w}\right) = (1-\alpha)\tilde{P}_{i,t}^{w} \le P_{i,t}^{w} \le (1+\alpha)\tilde{P}_{i,t}^{w} \tag{25}$$

where $\tilde{P}_{i,t}^{w}$ and $P_{i,t}^{w}$ denote the predicted and actual values of wind farm output and α denotes the corresponding fluctuation range. When the actual wind power output is lower than the predicted value, other conventional units or CHP provide insufficient power to meet the load demand, thereby increasing the total power costs.

$$P_{i,t}^{w} = (1-\alpha)\tilde{P}_{i,t}^{w} \tag{26}$$

where $0 \le \alpha \le 1$. Assuming that the increased cost cannot exceed $(1+\beta)f_0$ and that the range of β is $\beta \ge 0$, the following optimization models must be considered.

$$f \le (1+\beta) f_0 \tag{27}$$

In equation (27), when $f = (1+\beta) f_0$, the adverse disturbance is maximised. Therefore, the optimization model can be formulated as

$$\begin{cases} \max\limits_{X} \alpha \\ s.t.\ f \le (1+\beta) f_0 \\ \quad P_{i,t}^{w} = (1-\alpha)\tilde{P}_{i,t}^{w} \\ \quad G(X,\gamma) = 0 \\ \quad H(X,\gamma) \le 0 \\ \quad 0 \le \alpha \le 1, \qquad \beta \ge 0 \end{cases} \tag{28}$$

The above model indicates that if the wind power output fluctuates within the range of $\left[(1-\alpha)\tilde{P}_{i,t}^{w},\ \tilde{P}_{i,t}^{w}\right]$, then the value of objective function should not exceed $(1+\beta)f_0$.

3. SIMULATION ALGORITHMS

3.1 FOA

Fig. 2 presents the schematic diagram of FOA, which is developed based on the foraging behaviour of fruit flies. Fruit flies use their natural strong visual and olfactory abilities to search their surrounding space for the best next location until the best value is obtained. Based on this behaviour, the standard flow of FOA is formulated as shown in Fig. 3.

Compared with other optimization algorithms, FOA has fewer initial parameters, a simpler calculation process, can be easily converted into a programming language and can be easily understood. However, FOA also has a poor population diversity, low convergence accuracy and can easily fall into the local optimum. Given these problems, this paper proposes VD-FOA that effectively improves the convergence accuracy, speed and global search ability of the conventional FOA.

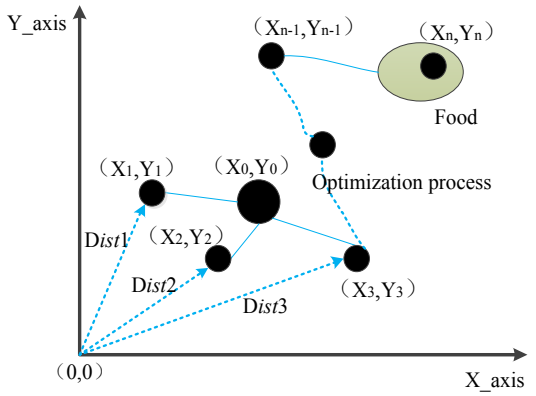

Fig. 2. Schematic diagram of FOA.

Step 1: Initialization population size, a maximum number of iterations, contraction parameter and the initial position of fruit fly population;
Step 2: Giving fruit fly individuals the random direction and distance to use their sense of smell to search for food. $X_i = X_0 + w*rand$;
Step 3: Estimating the distance between the origin and the individual of fruit fly $Dist$, calculate the smell concentration value to determine the value S_i;
Step 4: Calculating the smell concentration of individual location of fruit fly $Smell_i$;
Step 5: Finding out the individual with the optimal smell concentration value in the fruit fly population.;
Step 6: Retaining the optimal smell concentration and optimal position, moreover the fruit fly population flew to this position using a vision to form a new population position.
Step 7: Entering the iteration optimization and repeat steps 2 - 6 until the maximum number of iterations is reached.

Fig. 3. Standard fruit fly optimization algorithm flow

3.2 Visual-detection Based Fruit Fly Optimization Algorithm

This section presents the VD-FOA, which is illustrated in Fig. 4.

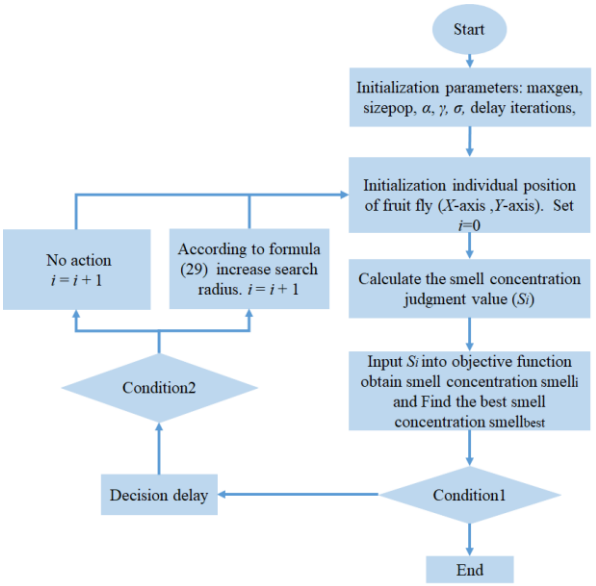

Fig. 4. Flow chart of VD-FOA.

$$w = \alpha * e^{\left(\frac{\max gen - i}{\max gen}\right)^{\gamma}} \tag{29}$$

where w is search radius, α denote contraction factor and γ = 2~6.

In Fig. 4, the judgment condition 1 denotes whether the maximum number of iterations has been reached. When this condition is satisfied, the optimization process is terminated and the optimal smell concentration is outputted; otherwise, the decision delay mechanism is executed. Meanwhile, the judgment condition 2 indicates whether the variance of the smell concentration value within the set number of delay iterations is less than the set value of the smell concentration variance (σ). If the condition is satisfied, no change is made to continue the iteration. If the condition is not satisfied, then the search radius is changed according to formula (29) and the iteration continues.

3.3 VD-FOA Performance Analysis

To test the effectiveness of the proposed algorithm, four standard test functions are selected as described in Table 1. The sizepop = 100, the maxgen = 1000 and delay iterations = 15, σ = 0.001, α = 40 and γ = 4. The test results in Table 2 reveal that the proposed VD-FOA is superior to the conventional FOA in terms of optimization accuracy. In addition, Fig. 5 shows that VD-FOA can reach the global optimum much faster compared with the traditional FOA. In sum, VD-FOA outperforms the conventional FOA.

Table 1. Four standard test functions

Serial number	Function name	Each dimension search area	Optimal function value

f_1	Sphere	[-100,100]	0
f_2	Step	[-100,100]	0
f_3	Griewank	[-600,600]	0
f_4	Rastrigin	[-5.12,5.12]	0

Table 2. Comparison of simulation results of two algorithms

Function	FOA	VD-FOA
f_1	5.21×10^{-7}	3.42×10^{-11}
f_2	5.16×10^{-7}	3.37×10^{-11}
f_3	1.17×10^{-5}	1.03×10^{-10}
f_4	1.03×10^{-4}	9.23×10^{-9}

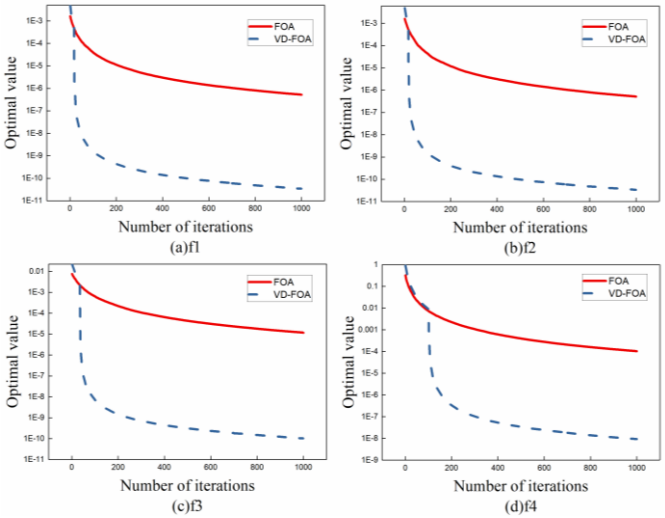

Fig. 5. The optimization process of FOA and VD-FOA algorithms.

4. CASE STUDIES

The validity of the proposed model is verified by using the IES, which includes the IEEE 24-node power network and the 20-node natural gas network as shown in Fig. 6. Four CHPs are located at nodes 1, 2, 16 and 22 of the system whilst the other units are conventional units. Three wind farms with capacities of 200, 150 and 100 MW are also connected to 8, 19 and 21 nodes. The two ES units at 19 and 21 nodes have SOC_{max} of 200 MW and 100 MW and charging/discharging efficiencies of 0.95 and 0.9. The other parameters are presented in (Soroudi, A,2017).

The six cases presented in Table 3 are examined to analyse the robustness of the IES and to study the effect of the ES unit and its SOC_{max} on the robustness of an IES with wind power. Fig. 7 presents the simulation results in these six cases.

Table 3. Six cases of robust analysis for IES

Case studies	SOC_{max} of ES unit (Node 19) /MW	SOC_{max} of ES unit (Node 21)/MW
Case 1	No ES unit	No ES unit
Case 2	150	50
Case 3	200	100
Case 4	200	150
Case 5	250	150
Case 6	300	200

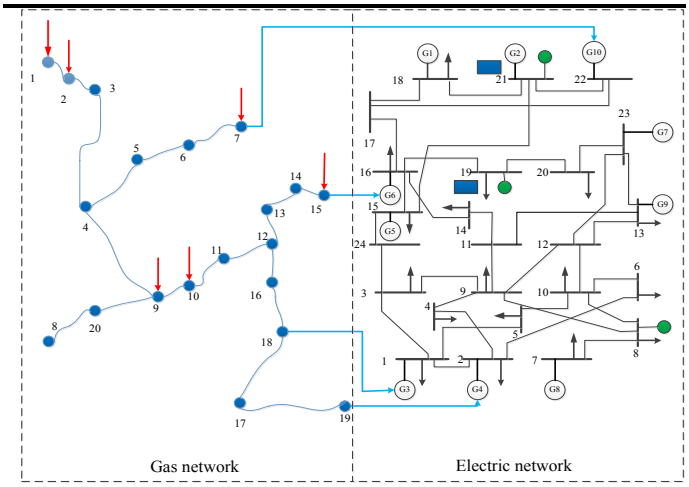

Fig. 6. Integrated energy system with gas-electric coupling.

In Fig. 7, α increases along with the deviation factor β, that is, the capacity of the system to absorb wind power continues to improve. When the value of β is kept the same, the ability of the IES to absorb wind power in Case 2 is stronger than that in Case 1 because the ES unit can rapidly transmit electric energy through the charging/discharging function. In this case, the ES unit meets the peak cut requirements and improves the robustness of the IES. As can be seen from Cases 2-6, the α increases with SOC_{max} and the robustness of the system is continuously improved, which can provide a basis for the allocation of the SOC_{max} for the decision maker within the range of tolerable operating costs. At the same time, it also ensures that the system has an ability to absorb uncertain wind power.

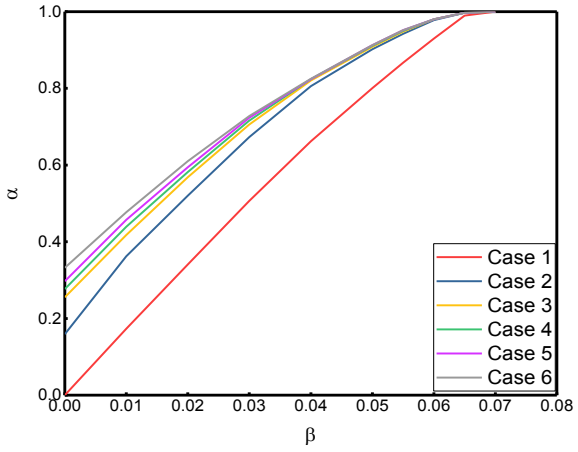

Fig. 7. Comparison of simulation results of six cases.

5. CONCLUSION

An effective Visual-detection based fruit fly optimization algorithm (VD-FOA) is proposed in this work for solving the information gap decision theory (IGDT) based robust analysis problem of integrated energy systems (IES). The VD-based decision delay and visual feature detection are integrated within the FOA. By using the decision delay and visual feature detection, VD-FOA changes the search radius

of fruit fly according to the variance of smell concentration. The proposed VD-FOA is tested by using standard test functions and the experimental comparison with the conventional FOA show the effectiveness of the proposed algorithm. The VD-FOA is also applied for the IGDT robust analysis of an IES. The IES integrated with ES unit can effectively deal with the uncertainty of wind power. The increase of the SOC_{max} can improve the robustness of the system accordingly.

6. REFERENCES

Alismail, F., Xiong, P., Singh, C. (2018). Optimal wind farm allocation in multi-area power systems using distributionally robust optimization approach. *IEEE Trans. Power Systems*, 33, (1), pp. 536-544.

Ben-Haim, Y. (2006). *Info-gap Decision Theory: Decisions under Severe Uncertainty*. Elsevier: Amsterdam.

Darvish, A., Ebrahimzadeh, A. (2018). Improved fruit-fly optimization algorithm and its applications in antenna arrays synthesis. *IEEE Trans. Antennas and Propagation*, 66, (4), pp. 1756-1766.

Dolatabadi, A., Jadidbonab, M., Mohammadi-ivatloo, B. (2019). Short-term scheduling strategy for wind-based energy hub: a hybrid stochastic/IGDT approach. *IEEE Trans. Sustainable Energy*, 10, (1), pp. 438-448.

Dongxiao, N., Tiannan, M., Bingyi, L. (2017). Power load forecasting by wavelet least squares support vector machine with improved fruit fly optimization algorithm. *Journal of Combinatorial Optimization*, 33, (3), pp. 1122-1143.

El-Ela, A. A. A., El-Sehiemy, R. A. A., Mouwafi, M. T., Salman, D. A. F. (2018). Multiobjective Fruit Fly Optimization Algorithm for OPF Solution in Power System.//2018 *Twentieth*.

Kampouropoulos, K., Andrade, F., Sala, E., Espinosa, A. G., & Romeral, L. (2018). Multiobjective optimization of multi-carrier energy system using a combination of ANFIS and genetic algorithms. *IEEE Trans. Smart Grid*, 9, (3), pp. 2276-2283.

Khaled, U., Eltamaly, A., M.; Beroual, A. (2017). Optimal power flow using particle swarm optimization of renewable hybrid distributed generation. *Energies*, 10,(7), 1013.

Mehdizadeh, A., Taghizadegan, N., Salehi, J. (2018). Risk-based energy management of renewable-based microgrid using information gap decision theory in the presence of peak load management. Appl. Energy, 2018, 211, pp. 617-630.

Mombeini, H., Yazdani-Chamzini A., Streimikiene D., & Zavadskas, E. K. (2018). New fuzzy logic approach for the capability assessment of renewable energy technologies: Case of Iran. *Energy & Environment*, 29, (4), pp. 511-532.

Nemati, M., Braun, M. (2018). Tenbohlen S. Optimization of unit commitment and economic dispatch in microgrids based on genetic algorithm and mixed integer linear programming. *Appl. Energy*, 210, pp. 944-963.

Niu, D., Wang, H., Chen, H. & Liang, Y. (2017). The general regression neural network based on the fruit fly optimization algorithm and the data inconsistency rate for transmission line icing prediction. *Energies*, 10, (12), 2066.

Nojavan, S., Majidi, M., Zare, K. (2017). Risk-based optimal performance of a PV/fuel cell/battery/grid hybrid energy system using information gap decision theory in the presence of demand response program. *International Journal of Hydrogen Energy*, 42, (16), pp. 11857-11867

Rabiee, A., Nikkhah, S., Soroudi, A .(2018). Information gap decision theory to deal with long-term wind energy planning considering voltage stability. *Energy*, 147, pp. 451-463.

Shudapreyaa, R. S., Anandamurugan, S. (2015). Parameter Selection Using Fruit Fly Optimization. *i-Manager's Journal on Computer Science*, 3, (4), 29.

Soroudi, A. (2017a). *Power System Optimization Modeling in GAMS*. Springer: Switzerland.

Stanislav, P., Bryan, K., Tihomir, M. (2009). Smart Grids better with Reset integrated energy system, *Electrical Power & Energy Conference (EPEC). IEEE*, pp. 1–8.

Tabar, V. S., Jirdehi, M. A., Hemmati, R. (2017). Energy management in microgrid based on the multi objective stochastic programming incorporating portable renewable energy resource as demand response option. *Energy*, 118, pp. 827-839.

Vahid-Pakdel, M. J., Nojavan, S., Mohammadi-Ivatloo, B., Zare, K. (2017). Stochastic optimization of energy hub operation with consideration of thermal energy market and demand response. *Energy Conversion and Management*, 145, pp. 117-128.

Xiong, P., Jirutitijaroen, P., Singh, C. (2016). A distributionally robust optimization model for unit commitment considering uncertain wind power generation. *IEEE Trans. Power Systems*, 32, (1), pp. 39-49.